A Fast Multiresolution Approach Useful for Retinal Image Segmentation

Dario Lo Castro[1], Domenico Tegolo[1,2] and Cesare Valenti[1]
[1]*Department of Mathematics and Computer Science, University of Palermo, via Archirafi 34, Palermo, Italy*
[2]*CHAB-Mediterranean Center for Human Health Advanced Biotechnologies, University of Palermo, Palermo, Italy*

Keywords: Elliptical Gaussian filters, Directional Map, Retinal Vessel, Fundus Oculi.

Abstract: Retinal diseases such as retinopathy of prematurity (ROP), diabetic and hypertensive retinopathy present several deformities of fundus oculi which can be analyzed both during screening and monitoring such as the increase of tortuosity, lesions of tissues, exudates and hemorrhages. In particular, one of the first morphological changes of vessel structures is the increase of tortuosity. The aim of this work is the enhancement and the detection of the principal characteristics in retinal image by exploiting a non-supervised and automated methodology. With respect to the well-known image analysis through Gabor or Gaussian filters, our approach uses a filter bank that resembles the "à trous" wavelet algorithm. In this contribution we show a particular approach to speed-up the computing time. This methodology rotates the kernels and it is a fast enough to extract information useful to assess vessel tortuosity and to segment (not considered explicitly in this paper) retinal images. Furthermore, we compare on the public databases DRIVE and DIARETDB0 our output images against the SCIRD-TS algorithm, which is considered as one of the most effective supervised methods for the detection of retinal thin structures.

1 INTRODUCTION

In the last two decades the retinal diseases research obtained great results in fundus oculi image analysis. Retinal image analysis ensures a non-invasive examination that shows many characteristics of microcirculation, due to a useful screening tool like videocapillaroscopy (Bellavia et al., 2014a). Recently, some scientific contributions highlight the correlation between coronary heart disease and coronary microvascular dysfunctions (McClintic et al., 2010). Information about fundus oculi features, from various methodologies, are valid and effective resources for the physician. Optic disk, macula, retinal vessels, hemorrhages, exudates, micro-aneurysm and tortuosity are quite important features and give information on eye health, more in general on cardiovascular circulation of the patient. Image processing automated techniques for blood vessels segmentation were developed in (Salazar-Gonzalez et al., 2014; Gupta et al., 2016; Lukac and Subasic, 2017). By exploiting Gabor filters, methodologies for measurement, tracking, detection and segmentation of the width of major temporal arcades were described in (Oloumi et al., 2015). In (Zhang and Zhao, 2016) we can find an approach that uses compactness, uniformity and local density to locate the optic disk. That methodology exploits bidimensional Gabor filters with a rotation angle at step of 15°. There are also methods based on tubular shape and geometrical models to highlight curvilinear structures (Annunziata et al., 2016; Soares et al., 2006). Instead, global and local directional models are used in (Wu et al., 2016) to identify the optic disk location by its brightness and parabolic shape. With respect to the detection of exudates an interesting approach was defined by Giancardo et al. (Giancardo et al., 2012) which introduces a method for diagnosis of diabetic retinopathy by using a set of features based on color, wavelet decomposition and segmentation of lesions. A promising approach based on keypoints (Bellavia et al., 2014b) was described in (Zhanga et al., 2015). In (Youssif et al., 2008) Youssif et al. present a method to detect the optic disk by the degree between vessel map and vessel's direction matched filter. Moreover, a circular brightness object was found by Lu and Lim in (Lu and Lim, 2011) in order to define a unique circular brightness structure of the optic disk. All these methods adopted a model to identify the right structures. A hand-crafted ridge detector, named SCIRD, was described in (Annunziata and Trucco, 2016), invariant to rotations, resizing and curvatures. This ap-

Lo Castro D., Tegolo D. and Valenti C.
A Fast Multiresolution Approach Useful for Retinal Image Segmentation.
DOI: 10.5220/0006579203400345
In *Proceedings of the 7th International Conference on Pattern Recognition Applications and Methods (ICPRAM 2018)*, pages 340-345
ISBN: 978-989-758-276-9

proach uses an appearance and context model, including multi-range learned filters, to extract a tubularity measure, obtained by convolving the image with second-order directional derivatives similar to a Gabor filter bank (Soares et al., 2006). In this way, that approach faces the problem of point-like and irregular structures. The drawback of that methodology is the fine-tuning of various parameters. SCIRD-TS, before of choosing the final values, requires to test various parameters, therefore spending so much training and computing time. In literature there are non-automated methods that needed a manual tuning, or an initial training step which is deeply subjected to the values of parameters proposed by the trainer. However, those methods should be considered non-supervised and non-automated as they require a long computing and processing time, because the a priori choosing of the input values.

Vice versa, our method, instead of the well-known Gabor filter approaches, uses an elliptical Gaussian filter bank in a way that resembles the "à trous" wavelet algorithm (Shensa, 1992), pre-calculated filters and without no particular tuning of parameters. Therefore it results faster with respect to the traditional methods that require a priori settings of the input parameters. For this reason, we consider our methodology as a non-supervised approach. Furthermore, we introduced a color directional map to assess better visually the retinal vessels tortuosity (Aghamohamadian-Sharbaf et al., 2016). In this contribution we carryed out a comparison against the output images obtained from SCIRD-TS by Annunziata et al (Annunziata and Trucco, 2016) on images with different resolutions and size from the well-known public databases DRIVE (Staal et al., 2004) and DIARETDB0 (Kauppi et al., 2012).

2 PROPOSED METHODOLOGY

In order to put in evidence both linear and curvilinear structures of retinal vessels (see figure 2) we preferred to use elliptical Gaussian filters with respect to the standard Gabor filters (Biran et al., 2016; Carnimeo et al., 2016; Fraz et al., 2017; Geetharamani and Balasubramanian, 2016; Kuri, 2015). In this way the vessel profile is matchable with the kernel one (see figure 1 and figure 2). To compute the filters bank we implemented the following function:

$$G(x,y,\sigma_x,\sigma_y,\mu_x,\mu_y) = \frac{e^{-\frac{(x-\mu_x)^2}{2\sigma_x^2}-\frac{(y-\mu_y)^2}{2\sigma_y^2}}}{2\pi\sigma_x\sigma_y} \qquad (1)$$

where $\mu_x = 0$ and $\mu_y = 0$ so that the center of the function coincides with the center of the kernel κ and where $\sigma_x = 0.8$ and $\sigma_y = 1.6$, determined experimentally, modulate the frequency along the main axis. Furthermore, we have that $x,y \in \{-2,-1,0,1,2\}$.

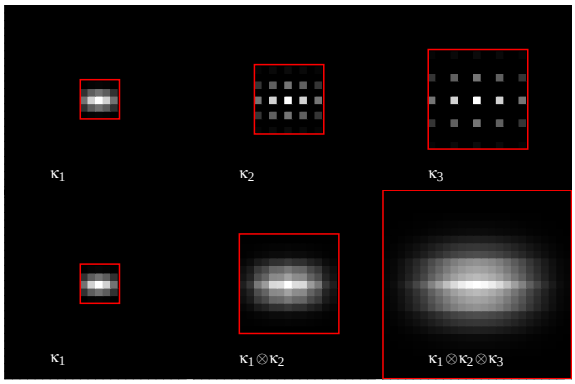

Figure 1: The sequence of convolutions with κ_1, κ_2 and κ_3 (which have the size 5×5, 9×9 and 13×13) is equivalent to single convolutions on the same image with kernels with size 5×5, 13×13 and 25×25. The overall shape of the elliptical Gaussian function is maintained.

Our methodology exploits the "à trous" approach (Shensa, 1992) (in French it means "with holes" due to the zero elements) to increase the processing velocity and to decrease the computing time (indeed the algorithm considers the same number of non-zero elements for every kernel). As in figure 1, starting from the 5×5 kernel κ, we added zero (i.e the holes) in order to enlarge κ, thus obtaining a bigger kernel κ_n

$$\kappa_n(nx,ny) = \kappa(x,y) \qquad (2)$$

where index n rules only the size of kernel, keeping the same number of non-zero elements unchanged. Starting from the 5×5 kernel, $\kappa_1 \equiv \kappa$, we have 25 non-zero elements, regardless to the size of the kernel of the filters bank. Unlike the original "à trous" algorithm, we set the distance between a kernel and its next bigger one does not grow up like a power of 2, because so we had kernels matchable with the width of retinal vessels in a more precise way.

Starting from a filters bank composed by 5×5 κ_1, 9×9 κ_2 and 13×13 κ_3 kernels (see top row of figure 1), by convolving every filter with the previous one, we obtained elliptical kernels (see bottom row figure 1)with 5×5, 13×13 and 25×25 sizes, respectively. This approach makes constant the computing time and achieves good results with respect to those with more time complexity. Furthermore, we wanted to make our approach invariant to rotations, thus to obtain and to extract the information about retinal vessels tortuosity. Unlike (Annunziata et al., 2016; Annunziata and Trucco, 2016; Zhang and Zhao, 2016)

which use an angle θ at step of 15° to overtake the time complexity problem due to convolutions, we rotated the kernels with a step of 2°, with an angle $\theta = [0^\circ, 178^\circ]$. In such a way we ensured a fine valuation of the vessel orientation. Furthermore, we did not analyze the results through neural networks and we did not apply any sub-sampling (Paranjape et al., 2015; Rizvi et al., 2016; Wang et al., 2017). At the end, we had a more general κ_n^θ and only three iterations and convolutions with the input (for every n and θ). Different directions and sizes of the kernels highlight in turn the various curvilinear structures of input image (see figure 3).

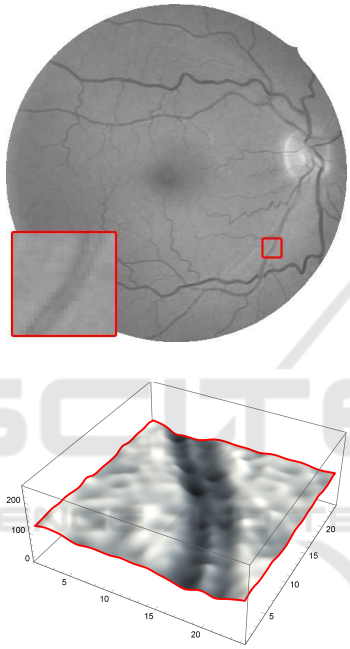

Figure 2: A zoomed detail of 24×24 pixels (gray levels interpolated and emphasized for better display purposes). The small central reflex, usually present along the vessel, can be matched by 5×5 elliptical Gaussian kernel.

Our approach, starting from the smallest 5×5 kernel convolved with the input image, for every rotation angle, subtract from the input image all highlighted structures. This process is repeated with bigger kernels in order to bigger always retinal structures. It must be noted how the smallest details are detected by κ_1^θ kernels even if normally they are considered noise, whereas wider vessels are enhanced by κ_3^θ. For the DRIVE and DIARETDB0 databases it is not necessary to use kernels bigger than κ_3^θ to match the vessel width. This approach, considering $\theta = [0^\circ, 178^\circ]$, locates vessels orientation, because the definitive direction corresponds to the maximum correlation value in that pixel, for the whole set of convolutions. By exploiting this information, we obtain a directional map of colors inspired by the HSV palette (see figure 4 and figure 5). To avoid any problem due the fact that even zones that do not present any vessel show a preferential color/direction, we exclude the background by multiplying the map by the maximum correlation value itself. The resulting direction is coherent with respect to the image; this approach is simple but stable and it does not require any intervention to reduce possible fluctuations (e.g. a median filter in post-processing (Guastella and Valenti, 2016)). We believe that the information about vessels orientations extracted from the directional map can be a useful tool for a possible segmentation step (Escorcia-Gutierrez et al., 2016; Hamad et al., 2014; Keivani and Pourghassem, 2015; Mookiah et al., 2015; Rotaru et al., 2015; Waheed et al., 2015) together with the vessels brightness. We also believe that the directional map can be used to assess globally and locally retinal vessels tortuosity (Khansari et al., 2017).

3 DATABASE AND EXPERIMENTAL RESULTS

We used our approach on the retinal images of two standard and well-known public databases: the Diabetic Retinopathy Database and Evaluation Protocol (DIARETDB0) (Kauppi et al., 2012) and the Digital Retinal Images for Vessel Extraction (DRIVE) (Staal et al., 2004). Both databases present retinal images with both pathologies and no pathologies, with different resolutions. DIARETDB0 consists of 130 retinal images, 110 contain various symptoms of diabetic retinopathy and 20 without any diseases; all of 130 were labeled by four experts to locate the presence of hemorrhages, exudates and micro aneurysms. DRIVE consists of 40 retinal images, 7 contain symptoms mild early diabetic retinopathy and 33 do not show any sign of diseases; all of 40 images were labeled by two experts and divided into test and training sets, containing 20 images each. DIARETDB0 has images of 1500×1152 pixels, whereas DRIVE has images of 768×584 pixels. Despite this, the bank of filters κ_1^θ, κ_2^θ and κ_3^θ were used to process both databases, matching the dimensions of fundus oculi structures in any case. To compare the results of our approach with SCIRD-TS (Annunziata and Trucco, 2016) we used the FSIM (Zhang et al., 2011) and Dice (Abirami et al., 2015) measures. In order to put in evidence the differences between these measures (FSIM evaluates the overall aspect of the images, whereas Dice performs a pixel-wise analysis) to evaluate the robustness of the proposed method we introduced Gaussian noise

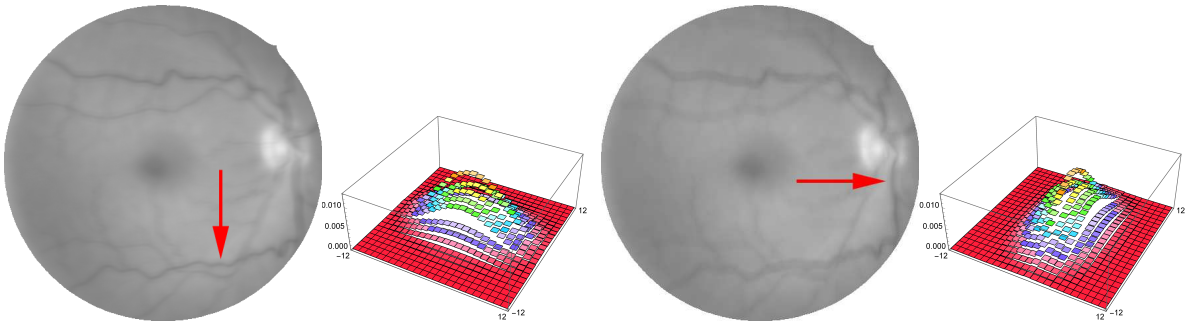

Figure 3: Graphic representation of convolutions with κ_1, κ_2 and κ_3 together, which corresponds to a 25×25 kernel.In general the bigger the kernel, the wider the detected components.Rotating the kernel allows to identify the orientation of the vessels (highlighted by the arrows in the case of horizontal and vertical targets).

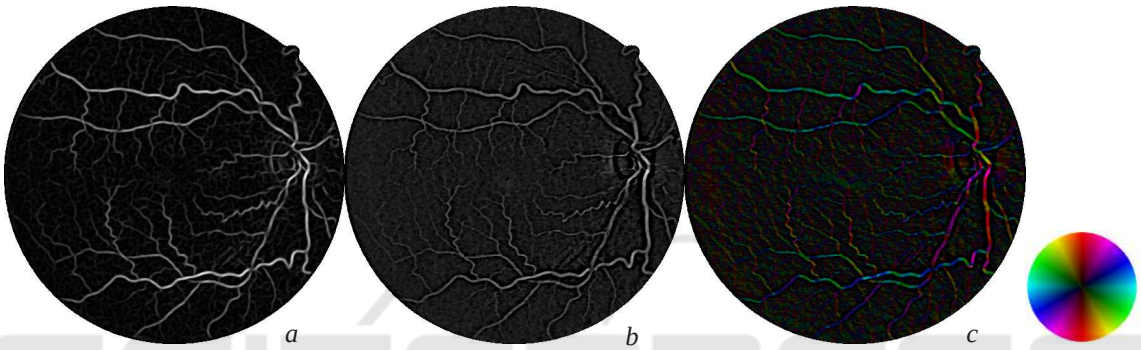

Figure 4: Qualitative comparison between the results obtained on the DRIVE input image (figure 2) by the algorithm described in (Annunziata and Trucco, 2016) (*a*) and our methodology (*b*).We produce also a direction map (*c*) whose hue indicates the orientation assigned to each pixel while the luminosity is extracted by the result itself (*c*).

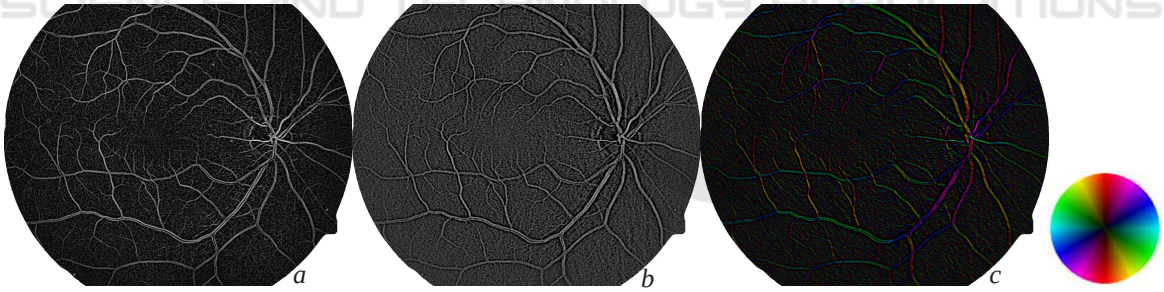

Figure 5: Qualitative comparison between the results obtained on a typical DIARETDB0 image by the algorithm in (Annunziata and Trucco, 2016) (*a*) and our methodology (*b*,*c*).

up to 30%, too. The FSIM measure uses the phase congruency to extract the characteristics and the gradient magnitude to code the contrast information and evaluates the feature similarities of the images on a local basis, as for the human visual system. Vice versa, the Dice measure compares pixel-by-pixel similarities of the images. For the input parameters of SCIRD-TS (freely distributed implementation available at http://staff.computing.dundee.ac.uk/rannunziata), we used its default values.

Average results are reported in figure 6 and in particular they show FSIM=0.88 and Dice=0.85 with respect to DRIVE and FSIM=0.89 and Dice=0.83 with respect to DIARETDB0. To verify the robustness of our method we also introduced a Gaussian noise with a step of 1% up to 30% in the input images (see figure 6). We have to point out that our methodology does not require any time in choosing the parameters, as opposed to the SCIRD-TS algorithm or as opposed to many other algorithms described in the literature. Our method is non-supervised, while it is only subject to the smallest κ_1 (which depends on the width

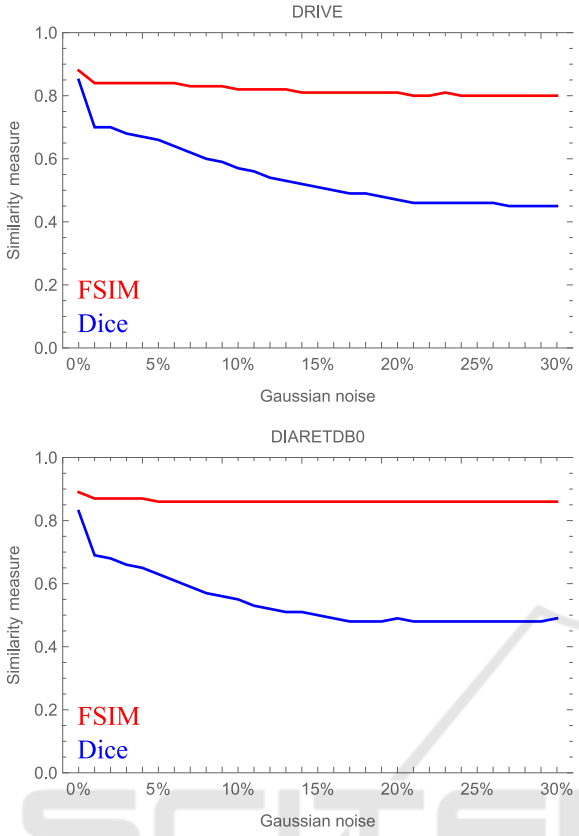

Figure 6: Average quantitative comparison through the FSIM and Dice measures between the output images obtained by the algorithm described in (Annunziata and Trucco, 2016) and our methodology, with respect to different amount of Gaussian noise.

of the smallest vessels). Our algorithm was developed in MatLab language without taking care of particular optimization tricks. In a low level language, thanks to the pre-computed bank of filters, our algorithm takes few seconds to process an image on an Intel Core i7-3770 CPU with 3.40 Ghz, 8.0 GB-RAM and a NVIDIA GeForce GT 620; therefore it should be useful in the case of a real time applications.

4 CONCLUSIONS AND FUTURE WORK

Our approach, despite its simplicity, is able to put in evidence and to enhance the retinal features and the prevalent directions of curvilinear and linear structures. The virtues of our methodology are: being a non-supervised approach; not having to tune parameters; minor computing time to process retinal images with respect to SCIRD-TS. We obtained good results in comparing our outputs and the SCIRD-TS ones. In the future work, we aim to decrease the complexity time by optimizing the code; to get a binary representation of the vessels by segmenting our output images; to use the color directional map to evaluate the vessels tortuosity.

REFERENCES

Abirami, S., Swapna, T., Pulari, S., and Chakraborty, C. (2015). Unsupervised segmentation of retinal vessels from fundus fluorescein angiogram images. *International Journal of Applied Engineering Research*, 10:38–43.

Aghamohamadian-Sharbaf, M., Pourreza, H., and Banaee, T. (2016). A novel curvature-based algorithm for automatic grading of retinal blood vessel tortuosity. *IEEE Journal of Biomedical and Health Informatics*, 20(2):586–595.

Annunziata, R., Kheirkhah, A., Aggarwal, S., Hamrah, P., and Trucco, E. (2016). A fully automated tortuosity quantification system with application to corneal nerve fibres in confocal microscopy images. *Med Image Anal*, 32:216–32.

Annunziata, R. and Trucco, E. (2016). Accelerating convolutional sparse coding for curvilinear structures segmentation by refining SCIRD-TS filter banks. *IEEE Trans Med Imag*, 35(11):2381–92.

Bellavia, F., Cacioppo, A., Lupaşcu, C., Messina, P., Scardina, G., Tegolo, D., and Valenti, C. (2014a). A non-parametric segmentation methodology for oral videocapillaroscopic images. *Computer Methods and Programs in Biomedicine*, 114(3):240–6.

Bellavia, F., Tegolo, D., and Valenti, C. (2014b). Keypoint descriptor matching with context-based orientation estimation. *Image and Vision Computing*, 32(9):559–67.

Biran, A., Bidari, P., Almazroa, A., Lakshminarayanan, V., and Raahemifar, K. (2016). Blood vessels extraction from retinal images using combined 2D Gabor wavelet transform with local entropy thresholding and alternative sequential filter. In *Canadian Conference on Electrical and Computer Engineering*. IEEE.

Carnimeo, L., Altomare, A., and Nitti, R. (2016). A combined preprocessing method for retinal vessel detection towards proliferative diabetic retinopathy screening. In *Advances in Artificial Life, Evolutionary Computation and Systems Chemistry*, pages 106–16. Springer.

Escorcia-Gutierrez, J., Torrents-Barrena, J., Romero-Aroca, P., Valls, A., and Puig, D. (2016). Interactive optic disk segmentation via discrete convexity shape knowledge using high-order functionals. *Frontiers in Artificial Intelligence and Applications*, 288:39–44.

Fraz, M., Jahangir, W., Zahid, S., Hamayun, M., and Barman, S. (2017). Multiscale segmentation of exudates in retinal images using contextual cues and ensemble classification. *Biomed Signal Process Control*, 35:50–62.

Geetharamani, R. and Balasubramanian, L. (2016). Retinal blood vessel segmentation employing image processing and data mining techniques for computerized retinal image analysis. *Biocybernetics and Biomedical Engineering*, 36(1):102–18.

Giancardo, L., Meriaudeau, F., Karnowski, T., Li, Y., Garg, S., Tobin, K., and Chaum, E. (2012). Exudate-based diabetic macular edema detection in fundus images using publicly available datasets. *Medical Image Analysis*, 16(1):216–26.

Guastella, D. and Valenti, C. (2016). Cartoon filter via adaptive abstraction. *Journal of Visual Communication and Image Representation*, 36:149–158.

Gupta, V., Sengar, N., and Dutta, M. K. (2016). Automated segmentation of blood vasculature from retinal images. In *2016 2nd International Conference on Communication Control and Intelligent Systems (CCIS)*, pages 81–84. IEEE.

Hamad, H., Tegolo, D., and Valenti, C. (2014). Automatic detection and classification of retinal vascular landmarks. *Image Analysis Stereology*, 33(3):189–200.

Kauppi, T., Kalesnykiene, V., Kamarainen, J., Lensu, L., Sorri, I., Kälviäinen, H., and Uusitalo, H. (2012). A framework for constructing benchmark databases and protocols for retinopathy in medical image analysis. In *Intelligent Science and Intelligent Data Engineering*, pages 832–843.

Keivani, M. and Pourghassem, H. (2015). A blood vessel segmentation algorithm in retinal images using morphological and spatial features. *International Journal of Imaging and Robotics*, 15(4):12–28.

Khansari, M., ONeill, W., Lim, J., and Shahidi, M. (2017). Method for quantitative assessment of retinal vessel tortuosity in optical coherence tomography angiography applied to sickle cell retinopathy. *Biomedical Optics Express*, 8:3796–3806.

Kuri, S. (2015). Automatic diabetic retinopathy detection using gabor filter with local entropy thresholding. In *Recent Trends in Information Systems*, pages 411–5. IEEE.

Lu, S. and Lim, J. (2011). Automatic optic disc detection from retinal images by a line operator. *IEEE Trans Biomed Eng*, 58(1):88–94.

Lukac, A. and Subasic, M. (2017). Blood vessel segmentation using multiscale hessian and tensor voting. In *40th International Convention on Information and Communication Technology, Electronics and Microelectronics*, pages 1534–1539. IEEE.

McClintic, B., McClintic, J., Bisognano, J., and Block, R. (2010). The relationship between retinal microvascular abnormalities and coronary heart disease: a review. *Am J Med*, 123(4):1–7.

Mookiah, M., Tan, J., Chua, C., Ng, E., Laude, A., and Tong, L. (2015). Automated characterization and detection of diabetic retinopathy using texture measures. *J Mech Med Biol*, 15(4).

Oloumi, F., Rangayyan, R., Casti, P., and Ells, A. (2015). Computer-aided diagnosis of plus disease via measurement of vessel thickness in retinal fundus images of preterm infants. *Comput Biol Med*, 66:316–29.

Paranjape, S., Ghosh, S., Ray, A., and Chatterjee, J. (2015). Segmentation of retinal blood vessels through Gabor features and ANFIS classifier. In *International Conference on Industrial Instrumentation and Control*, pages 512–6. IEEE.

Rizvi, S., Cabodi, G., Gusmao, P., and Francini, G. (2016). Gabor filter based image representation for object classification. In *International Conference on Control, Decision and Information Technologies*, pages 628–632. IEEE.

Rotaru, F., Bejinariu, S., Luca, R., and Niţă, C. (2015). Retinal vessel labeling method. In *E-Health and Bioengineering Conference*, pages 1–4. IEEE.

Salazar-Gonzalez, A., Kaba, D., Li, Y., and Liu, X. (2014). Segmentation of the blood vessels and optic disk in retinal images. *IEEE Journal of Biomedical and Health Informatics*, 18:1874–1886.

Shensa, M. (1992). The discrete wavelet transform: wedding the à trous and Mallat algorithms. *IEEE Trans Sig Process*, 40(10):2464–82.

Soares, J., Leandro, J., Cesar, R., Jelinek, H., and Cree, M. (2006). Retinal vessel segmentation using the 2-d gabor wavelet and supervised classification. *IEEE Trans Med Imag*, 25(9):1214–22.

Staal, J., Abramoff, M., Niemeijer, M., Viergever, B., and van Ginneken, B. (2004). Ridge based vessel segmentation in color images of the retina. *IEEE Trans Med Imag*, 23(4):501–9.

Waheed, A., Akram, M., Khalid, S., Waheed, Z., Khan, M., and Shaukat, A. (2015). Hybrid features and mediods classification based robust segmentation of blood vessels. *J Med Syst*, 39(10).

Wang, Y.-B., Zhu, C.-Z., Yan, Q.-F., and Liu, L.-Q. (2017). A novel vessel segmentation in fundus images based on SVM. In *International Conference on Information System and Artificial Intelligence*, pages 390–4. IEEE.

Wu, X., Dai, B., and Bu, W. (2016). Optic disc localization using directional models. *IEEE Trans Image Process*, 25(9):4433–42.

Youssif, A., Ghalwash, A., and Ghoneim, A. (2008). Optic disc detection from normalized digital fundus images by means of a vessels direction matched filter. *IEEE Trans Med Imag*, 27(1):11–8.

Zhang, D. and Zhao, Y. (2016). Novel accurate and fast optic disc detection in retinal images with vessel distribution and directional characteristics. *IEEE J Biomed Health Inform*, 20(1):333–342.

Zhang, L., Zhang, L., Mou, X., and Zhang, D. (2011). FSIM: A feature similarity index for image quality assessment. *IEEE Trans Image Process*, 20(8):2378–86.

Zhanga, L., Fisherb, M., and Wang, W. (2015). Retinal vessel segmentation using multi-scale textons derived from keypoints. *Comput Med Imaging Graph*, 45:47–56.